Dynamic strengths of molecular anchoring and material cohesion in fluid biomembranes

2000 J. Phys.: Condens. Matter 12 A315

(http://iopscience.iop.org/0953-8984/12/8A/341)

J. Phys.: Condens. Matter **12** (2000) A315–A320. Printed in the UK PII: S0953-8984(00)07726-2

Dynamic strengths of molecular anchoring and material cohesion in fluid biomembranes

Evan Evans and Florian Ludwig

Departments of Physics and Pathology, University of British Columbia, Vancouver, BC, Canada

E-mail: evans@physics.ubc.ca

Received 13 September 1999

Abstract. Building on Kramers' theory for reaction kinetics in liquids and using laboratory experiments, we show how strengths of molecular anchoring and material cohesion in fluid-lipid membranes increase with rate of force and tension loading. Expressed on a scale of log(loading rate), the dynamic spectra of pull-out forces and rupture tensions image the microscopic and mesoscopic energy barriers traversed in molecular extraction and membrane failure. To capture such images, we have pulled single molecules from membranes with force rates from 1 to 10^4 pN s^{-1} and ruptured giant membrane vesicles with tension rates from 10^{-2} to 10^2 mN m^{-1} s^{-1}.

1. Introduction

Beyond intimate covalent links within protein and lipid molecules, biomembrane structure is mainly fluid and held together by weak hydrophobic interactions. Because of thermal activation, a molecule can be uprooted from the interface by any level of force and a membrane can open up a fatal hole under any level of tension when stressed for a sufficient length of time. Modelled as bound states confined by simple energy barriers, we show how strengths of molecular anchoring and material cohesion are tied to time through universal functions of loading rate (force/time or tension/time). Correlating these universal functions with recent experiments, we demonstrate that dynamic force and tension spectroscopies can reveal both microscopic and mesoscopic barriers which anchor molecules and impede nucleation of holes in fluid membranes.

2. Theory

The connection between strength and survival of weakly bonded structures follows from the physics developed by Kramers [1] 60 years ago to describe kinetics of chemical reactions. Overdamped in condensed liquids, kinetics of unbinding reduce to diffusive transport of thermalized states (Smoluchowski theory) from a deep energy minimum outward—past a barrier—via a saddle point in the energy landscape [2]. There can be many such paths with complex trajectories in configuration space. However, application of an external field or load L (force f or tension σ_m) acts to select a reaction path, which can then be represented by a scalar coordinate x. Analysed along this coordinate, the outcome is a generic expression for

unbinding rate $k_>$ that depends on how the energy landscape $E(x)$ is deformed by the external load [3],

$$k_> = (D/l_c l_{ts}) \exp[-E_b(L)/k_B T].$$

The diffusive dynamics define an attempt frequency $D/l_c l_{ts}$, or diffusion time $t_D = l_c l_{ts}/D$, governed by viscous damping $\gamma = k_B T/D$ and two length scales. The length l_c is the thermal spread defined by the rise in energy $\Delta E_c(x)$ local to the bound state, $l_c = \int \mathrm{d}x \exp[-\Delta E_c(x)/k_B T]$. The length l_{ts} is the energy-weighted width of the barrier defined by the fall in energy $\Delta E_{ts}(x)$ local to the transition state, $l_{ts} = \int \mathrm{d}x \exp[\Delta E_{ts}(x)/k_B T]$. In harmonic approximations, these lengths are derived from local curvatures $\kappa = (\partial^2 E/\partial x^2)$ of the energy landscape (e.g. $l_{ts} \sim (2\pi k_B T/\kappa_{ts})^{1/2}$). The major impact of load arises from changes in the thermal likelihood of reaching the top of the energy barrier, i.e. $\exp[-E_b(L)/k_B T]$ where $E_b(L)$ describes how the energy barrier depends on load.

Governed by exposure of hydrocarbon to water, the energy landscape for molecular anchoring in lipid bilayers is assumed to rise linearly along the normal to the membrane and end with a sharp energy barrier at $x = x_{ts}$ set by molecular length. Under force, a sharp barrier diminishes as $E_b(f) = E_b^0 - f x_{ts}$, which leads to exponentiation of rate on the scale of $f_\beta = k_B T/x_{ts}$,

$$k_> = 1/t_0 \exp(f/f_\beta)$$

(first postulated by Bell [4] to describe breakage of adhesion bonds). The prefactor, $1/t_0 = 1/t_D \exp(-E_b^0/k_B T)$, is a force-free rate governed by the initial barrier height E_b^0 and Kramers' classic result [1] for attempt frequency, $1/t_D = (\kappa_c \kappa_{ts})^{1/2}/2\pi\gamma$.

Analogous to opening a cavity in a 3D liquid, edge energy ε and lateral tension σ_m for a membrane hole play the roles of liquid surface tension and negative pressure in classical nucleation theory [5]. Defined in hole radius space, a soft energy barrier arises that moves inward, narrows and diminishes progressively with tension, i.e. $x_{ts} = \varepsilon/\sigma_m$, $l_{ts} \approx (2\pi k_B T/\sigma_m)^{1/2}$, $E_b(\sigma_m) = E_b^0 + \pi\varepsilon^2/\sigma_m$. As such, the failure rate grows rapidly on a scale set by $\sigma_\beta = \pi\varepsilon^2/k_B T$,

$$k_> = 1/t_0 (\sigma_m/\sigma_\beta)^{1/2} \exp(-\sigma_\beta/\sigma_m)$$

(first derived by Deryagin and Gutop [5] to describe breakdown of thin liquid films). In the prefactor, $1/t_0 = 1/t_D \exp(-E_b^0/k_B T)$, a Boltzmann weight is introduced to reflect formation of collective precursor states (e.g. curved indentations—[6]), which then open up as holes. The mesoscopic frequency $1/t_D$ scales as $\sim(\varepsilon^2/k_B T)/\gamma$ from theory but also depends nontrivially on membrane size. At large tension, the barrier location x_{ts} should collapse to a microscopic cut-off set by molecular radius and the height begin to decrease in proportion to load as for molecular unbinding.

Since forces and tensions increase with time in laboratory experiments, a first-order Markov equation is used to predict probability densities $p(t)$ for extraction or rupture events [3]. When parametrized by loading rate ($r_f = \Delta f/\Delta t$ and $r_\sigma = \Delta\sigma_m/\Delta t$), the distributions of times for events become distributions of force or tension $p(L)$. The peak in a distribution defines the load L^* for most frequent extraction or rupture (i.e. *strength*) and the relation of strength to loading rate is derived from $\partial p/\partial L = 0$,

$$[k_>]_{L=L^*} = r_L [\partial \log_e(k_>)/\partial L]_{L=L^*}.$$

Similarly, $-[1/p(L)][\partial^2 p(L)/\partial L^2]_{L=L^*}$ provides a measure of the variance ΔL^2. Both strength L^* and spread $\sim\Delta L$ are dynamical variables governed by thermal activation.

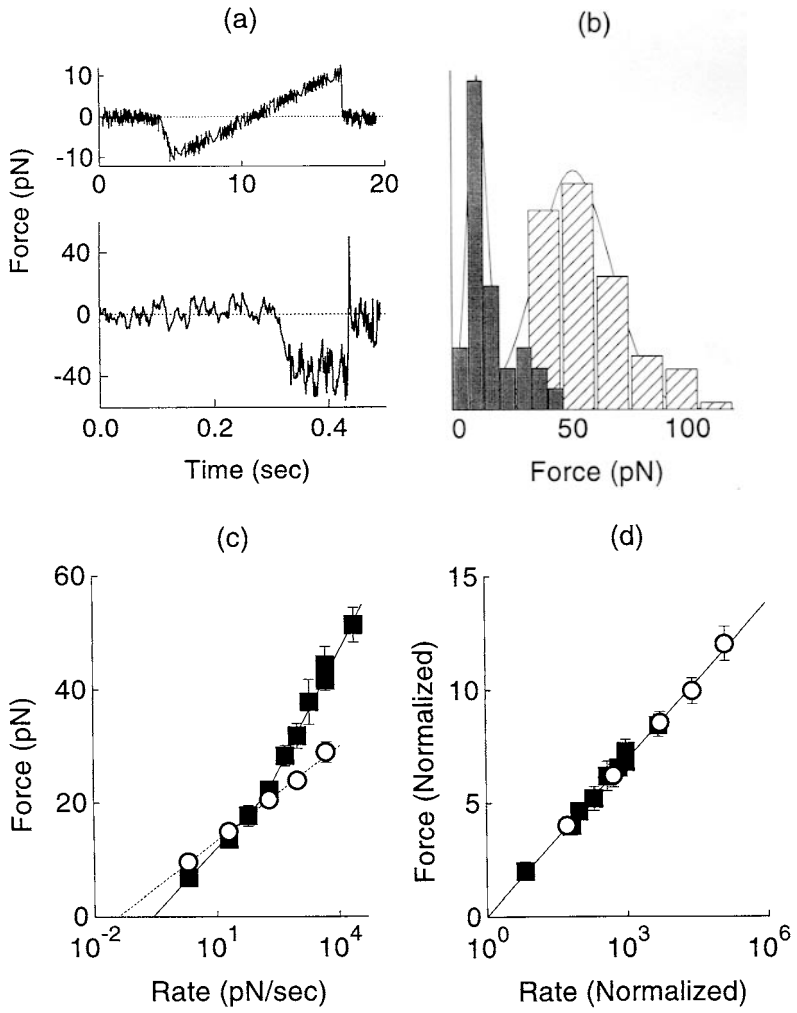

Figure 1. (a) Force versus time for probe approach to a bilayer vesicle surface (zero force), soft touch on contact (small negative force), then retraction with a test lipid attached to the tip (positive force) at slow and fast speeds until extraction (force recoils to zero). (b) Force histograms for slow $\sim$2 pN s^{-1} (left) and fast $\sim$25 000 pN s^{-1} (right) loading rates. (c) Spectra of anchoring strengths versus log(loading rate) measured for extraction of a diC18:0 test lipid from SOPC (closed boxes) and mixed SOPC:CHOL lipid bilayers (open circles). (d) Anchoring strength versus log(loading rate) on a universal scale set by thermal force f_β and loading rate r_β.

Introducing the kinetic rate $k_> \sim \exp(f/f_\beta)$ in the relation $[k_>]_{L=L^*}$ above shows that the most likely detachment force f^* impeded by a sharp energy barrier follows a universal logarithmic dependence on loading rate $r_f = \Delta f/\Delta t$ [3],

$$f^*/f_\beta = \log_e(r_f/r_\beta)$$

when normalized by thermal scales for force f_β and loading rate $r_\beta = f_\beta/t_0$. The spread in force is independent of rate, $\Delta f/f_\beta = 1$. Barrier energy and attempt frequency govern the intercept $r_f = r_\beta$ at zero force, $\log_e(r_\beta) = -E_b^0/k_BT + \log_e(f_\beta/t_D)$.

Introducing the kinetic rate $k_> \sim (\sigma_m/\sigma_\beta)^{1/2}\exp(-\sigma_\beta/\sigma_m)$ for hole nucleation in the relation $[k_>]_{L=L^*}$ also leads to a universal form for membrane strength σ_m^* as a function of loading rate $r_\sigma = \Delta\sigma_m/\Delta t$ approximated by

$$\sigma_\beta/\sigma_m^* \approx \tfrac{5}{2}\log_e(\sigma_m^*/\sigma_\beta) - \log_e(r_\sigma/r_\beta)$$

when scaled by thermal tension σ_β and loading rate $r_\sigma = \sigma_\beta/t_0$. The spread in rupture tension grows as $\Delta\sigma_m/\sigma_\beta \approx (\sigma_m^*/\sigma_\beta)^2/(1+3\sigma_m^*/\sigma_\beta)^{1/2}$ for $\sigma_m^*/\sigma_\beta < 1$. At very slow loading rates, the slope of reciprocal tension $1/\sigma_m^*$ versus $\log_e$ (loading rate) approaches the reciprocal thermal scale $k_BT/\pi\varepsilon^2$. At large tensions beyond the microscopic cut-off, a cross over is expected to a linear regime of membrane strength versus log(loading rate).

3. Experiments and discussion

3.1. Molecular anchoring in fluid membranes

To test anchoring strength, we prepared giant lipid bilayer vesicles (20–40 μm diameter) doped at extremely low concentration (<0.0001 mole fraction) with a special biotinylated test lipid. The hydrocarbon chains of the test lipid were the same length as the predominate membrane constituent, stearoyl–oleoyl phosphatidylcholine SOPC (C18:0/1) which in some cases was mixed l:l with cholesterol (CHOL). A biomembrane force probe BFP [7] decorated with streptavidin protein was used to attach—and then extract—test lipids from the vesicle bilayers under controlled ramps of force (figure 1(a)). To ensure (>90% confidence) extraction of single molecules, attachment frequency was limited to one per seven to ten contacts. Hundreds of repeated touches were needed to compile histograms of ∼50–100 extraction forces at each loading rate (figure 1(b)). Spectra of anchoring strengths versus log(loading rate) for SOPC and SOPC:CHOL bilayers are plotted in figure 1(c). Finding slopes and intercepts of linear regimes, we establish thermal scales for force f_β and loading rate r_β that map barriers to thermally averaged positions $x_\beta = \langle x_{ts}\cos\theta\rangle$ along the direction of force and define the characteristic rates $1/t_0$ for each barrier as listed in table 1.

Table 1. Thermal activation parameters for molecular unbinding.

Lipid bilayer	f_β (pN)	r_β (pN s^{-1})	x_β (nm)	$1/t_0$ (s^{-1})
SOPC (C18:0/1)	3.4 (6.1)	0.3 (5.2)	1.2 (0.7)	0.09 (0.9)
SOPC:CHOL (1:1)	2.4	0.04	1.7	0.016

Over the full range of rates, anchoring strength in SOPC:CHOL bilayers is governed by a single energy barrier. On the other hand, a second inner barrier (noted by parentheses in table 1) enhances anchoring strength on fast time scales in SOPC bilayers, which correlates with the position of the unsaturated bond in the oleoyl chain. Consistent with the concept of hydrophobic interaction, locations of the outermost barriers are comparable to half thicknesses of the hydrocarbon regions. Because of the small thermal force set by hydrophobic thickness, anchoring strengths are very weak unless molecules are extracted extremely rapidly.

3.2. Rupture of fluid membranes

To test rupture strength, giant fluid-bilayer vesicles were aspirated by micropipette and pressurized by a ramp of suction. For a fluid bilayer, tension is uniform over the vesicle surface and directly proportional to suction multiplied by pipette radius [8]. Examples of tension histories and rupture events are shown in figures 2(a), (b). Plotted versus log(loading

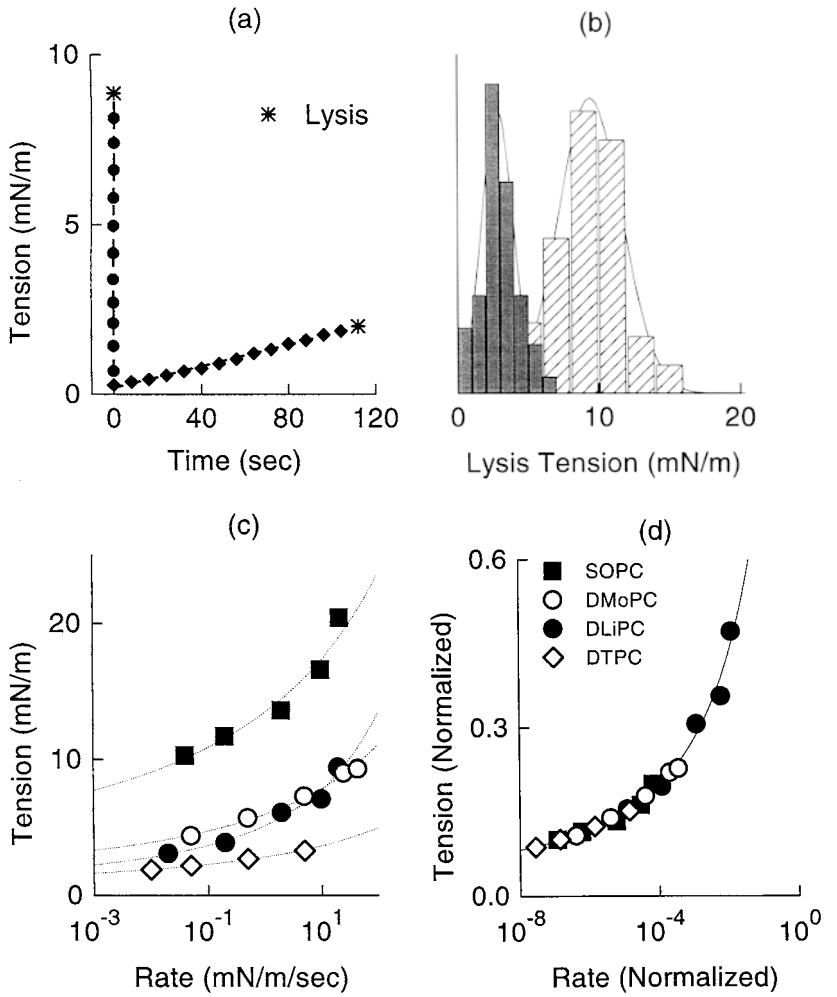

Figure 2. (a) Tension versus time for slow and fast micropipette pressurization of two lipid bilayer vesicles up to lysis (*). (b) Histograms of rupture tensions for slow 0.02 mN m^{-1} s^{-1} (left) and fast 20 mN m^{-1} s^{-1} (right) loading. (c) Rupture strength versus log(loading rate) measured for four types of PC lipid bilayer. (d) Membrane strength versus log(loading rate) on a universal scale set by thermal tension σ_β and loading rate r_β for each type of lipid bilayer.

rate) in figure 2(c), rupture tensions of PC bilayers with different acyl chains increase slowly over a nearly 10 000-fold range in rate and differ several-fold in level of strength. Correlating strength versus log(loading rate) with the universal theory (figure 2(d)), we obtain thermal tension σ_β and loading rate r_β scales and, thereby, edge energies ε and frequency prefactors $1/t_0$ for each PC bilayer as listed in table 2.

Interestingly, edge energies for these PC bilayers follow a scale proportional to membrane bending rigidity which seems to indicate that curved indentations or invaginations diminish hydrophobic exposure and reduce the edge energy as proposed many years ago [6, 9]. Although collective indentations may lower edge energy, the energy of formation E_b^0 is expected to be large, which could account for the significant variation in frequency scale $1/t_0$. Most intriguing, critical radii x_{ts} predicted by ε/σ_m only range from 1 to 2 times the radius of a PC molecule

Table 2. Thermal activation parameters for membrane rupture.

Lipid bilayer	σ_β (mN m^{-1})	r_β (mN m^{-1} s^{-1})	ε (pN)	$1/t_0$ (s^{-1})
DLiPC (diC18:2)	20	1.6×10^3	5.1	80
DTPC (diC13:0)	22	3.7×10^5	5.3	2×10^4
DMoPC (diC14:1)	41	1.2×10^5	7.3	3×10^3
SOPC (C18:0/1)	102	3×10^5	11.5	3×10^3

($\sim$0.5 nm) over the full range of tensions, which poses the question of why the continuum model of nucleation is so successful in modelling dynamic rupture of fluid membranes. Since the time scale for survival under tension is $\sim \exp[-\pi(\varepsilon/k_BT)x_{ts}]$, the obvious feature is that rupture only becomes likely once the critical radius approaches molecular dimensions ($\sim$nm) given these edge energies of 1 to 3 k_BT nm^{-1} ($k_BT \approx 4$ pN nm at room temperature). So under dynamic loading, rupture events below the peak in the tension distribution are likely to be governed by collective behaviour, whereas beyond the peak events are likely to reflect microscopic peculiarities.

Acknowledgments

The authors are grateful to Wieslawa Rawicz for expert technical assistance. This work was supported by a grant from the Medical Research Council of Canada (to EE), a graduate fellowship from Boehringer Ingelheim Fonds (to FL) and the Canadian Institute for Advanced Research Program in *Science of Soft Surfaces and Interfaces*.

References

[1] Kramers H A 1940 *Physica* **7** 284–304
[2] Hanggi P, Talkner P and Borkovec M 1990 *Rev. Mod. Phys.* **62** 251–342
[3] Evans E and Ritchie K 1997 *Biophys. J.* **72** 1541–55
[4] Bell G I 1978 *Science* **200** 618–27
[5] Zeldovich J B 1943 *Acta Physicochim. URSS* **18** 1–22
Deryagin B V and Gutop Y V 1962 *Kolloidn. Zh.* **24** 370–4
[6] Glaser R W, Leikin S L, Chernomordik L V, Pastushenko V F and Sokirko A I 1988 *Biochim. Biophys. Acta* **940** 275–87
[7] Merkel R, Nassoy P, Leung A, Ritchie K and Evans E 1999 *Nature* **397** 50–3
[8] Bloom M, Evans E and Mouritsen O G 1991 *Q. Rev. Biophys.* **24** 293–397
[9] Litster J D 1975 *Phys. Lett.* A **53** 193–4